

CHAPTER 1

INTRODUCTION

1.1 Background of Study

A gas turbine is a rotary mechanical device that extracts energy and converts it into useful work [1][4]. According to *H.I.H. Saravanamuttoo et al.* [1], it consists of an upstream rotating compressor coupled to a downstream turbine, and a combustion chamber in between. In the combustor, energy is added to the gas stream where fuel is mixed with air and ignited. The combustion of the fuel will raise the temperature in the high pressure environment of the combustor. Then, the product of the combustion will be forced into the turbine section. In the turbine section, the high volume and velocity of the gas flow will be directed through a nozzle over the turbine's blades, turning the turbine which powers the compressor and produces a certain net power. A reduction in the temperature and pressure of the exhaust gas will result in the energy given up to the turbine [1][4].

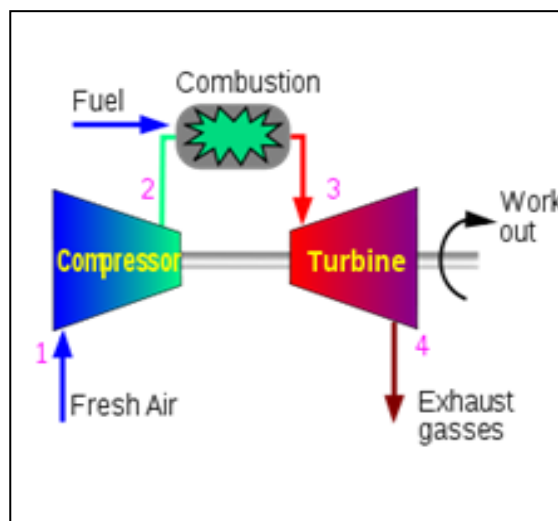


Figure 1.1: Basic principles of Gas Turbine; Brayton Cycle [1]

One of the important equipment in a gas turbine is the turbine blade [2][3][5]. *Boyce et al.* [2] claimed that turbine blades are exposed to thermal and centrifugal stress which results in a certain deformation and microstructure change as the usage time increases. This deformation is called creep. Microstructure change and creep affect

the turbine performance or may lead to catastrophic failure. Consequently, the blades life is limited. The search for a perfect method to predict the remaining creep life of used gas turbines blades has lead to the development of many equations used to extrapolate the results from High Temperature Creep Testing experiment, namely Stress-Rupture test [6][7]. Stress-Rupture test is the sudden and complete failure of a material held under a definite constant load for a given period of time at a specific temperature. *Walls et al.* [11] stated that one of the equations is the Life Fraction rule proposed by Robinson [11]. This equation will give approximation on the remaining creep life of the service-exposed turbine blades [11]. Thus, it will be easier to predict the remaining useful life. Furthermore, *Walls et al.* [11] also stated that the Stress-Rupture test result will be further develop to obtain the Larson-Miller parameter [11]. The Larson-Miller parameter will be compared with the one given by the manufacturer to draw a comparison. Thus, the different information will be evaluated. Other than that, *Smith et al.* [8] claimed that there will be microstructure changes on blade material after exposed to high stress and temperature over a long period of time. This is the main reason why the blades has limited service life. The difference between the unexposed and exposed service blades microstructure arrangement can be observed by using the Field Emission Scanning Electron Misroscope (FESEM) [8].

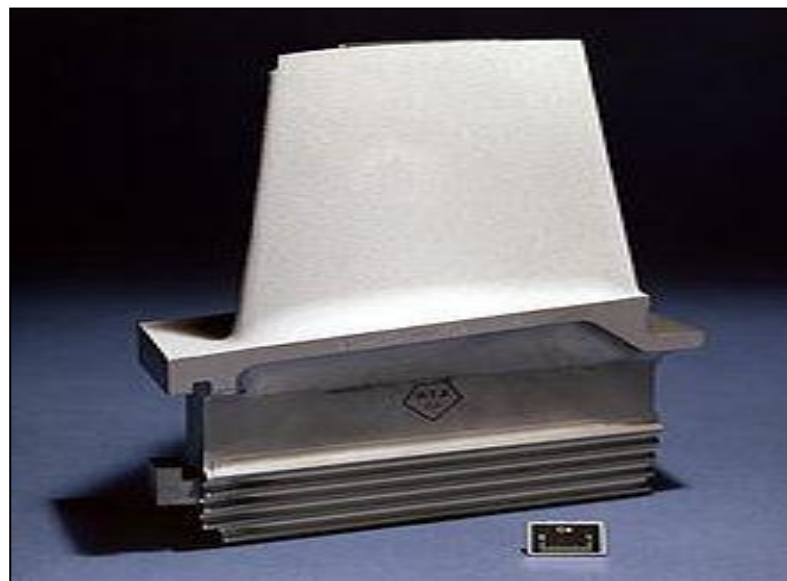


Figure 1.2: Turbine Blade [1]

1.2 Problem Statement

Materials used for high temperature purpose such as gas turbine blade will reach a certain deformation (creep) period after regularly use. This leads to a certain lifetime service of the components because of the limited service life of the material. Usually, the manufacturer will specify the expected useful life of the gas turbine blades. However, not all blades are deformed at the end of the expected useful life period. If those blades still can be used, replacing them will be a waste of capital. So, if it is possible to predict the remaining creep life of service-exposed blades, we can reuse thus saving the cost on new replacement blades. The samples were supplied by Malaysia Liquefied Natural Gas (MLNG) Labuan.



Figure 1.3: GE Gas Turbine blades from MLNG, Labuan

1.3 Objective of the Study

The main objectives of this study are:

- To determine the remaining creep life of a used gas turbine blades using Larson-Miller parameter and Life Fraction rule
- To investigate the microstructure change of used gas turbine blades at different service times

1.4 Scope of Study

This study will focus on:

- Samples preparation for the blades' microstructure examination
- Examination of the blades' microstructure using Field Emission Scanning Electron Microscope (FESEM)
- Determination of the remaining creep life of used gas turbine blades using Larson-Miller parameter and Life Fraction Rule

1.5 Relevancy of the Project

This project is relevant to the author as a Mechanical Engineering student who had completed courses related to industry such as Thermodynamics I, Thermodynamics II, Heat Transfer, and Energy Conversion and Management. Furthermore, it is very important to predict the remaining creep life of used gas turbine blades. This is because the capital cost could be saved on new blade replacement if it still can be used. Hopefully, this project will be beneficial financially for MLNG Labuan.

1.6 Feasibility of the Project within the Scope and Time Frame

There were two semesters of studies given to complete the Final Year Project. There are Final Year Project I and Final Year Project II for each semester. The time given was about eight months for the author to complete and document the project. During Final Year Project I, the author spent most of the time to do research on journals that are related to the project. Meanwhile, during Final Year Project II, the author has conducted the major part of the project which is the laboratory test for designed experiment. After all, the author will finally implement all the theories and knowledge he obtained from the laboratory research and provide conclusion for the project that will be finalized in a Final Year Project Report.

CHAPTER 2

LITERATURE REVIEW

2.1 Gas Turbine

The Table 2.1 shows the chronology of Gas Turbine development:

Table 2.1: Gas Turbine chronology [2]

Date	Name	Invention
130BC	Hero of Alexandria	Reaction Steam Turbine
1550	Leonardo da Vinci, Italy	Smoke Mill
1629	Giovanni Branca, Italy	Impulse Steam Turbine
1791	John Barber, England	Steam Turbine and Gas Turbine
1831	William Avery, USA	Steam Turbine
1837	M. Bresson	Steam Turbine
1850	Fernimough, England	Gas Turbine
1872	Dr. Stolze, Germany	Gas Turbine
1884	Charles A. Parsons	Reaction Steam Turbine & Gas Turbine
1888	Charles G.P. de Laval	Impulse Steam Turbine Branca type
1894	Armengaud+Lemale, France	Gas Turbine
1895	George Westinghouse	Steam Turbine Rights
1896	A.C. Rateau, France	Multi Impulse Steam Turbine
1896	Charles Curtis	Velocity Compound Steam Turbine/Gas Turbine
1895	Dr. Zoelly, Switzerland	Multi Impulse Steam Turbine
1900	F. Stolze, Germany	Axial Compressor & Turbine Gas Turbine
1901	Charles Lemale	Gas Turbine
1902	Stanford A. Moss, USA	Turbo-Charger/Gas Turbine
1903	A. Elling	Gas Turbine
1903	Armengaud+Lemale	Gas Turbine
1905	Brown Boveri	Gas Turbine
1908	Karavodine	Gas Turbine with deLaval Steam Turbine
1908	Holzwarth	Gas Turbine with Curtis + Rateau Compressor
1930	Frank Whittle, England	Aero Gas Turbine (Jet Engine)
1938	Brown Boveri—Neuchatel, Switzerland	1st Commercial Axial Compressor & Turbine

2.2 Gas Turbine System

The gas turbine cycle is explained by the Brayton Cycle. The characteristics of the operating cycle are shown on the pressure-volume map and the temperature-entropy map. The gas turbine, as a continuous flow machine, is best described by the first law of thermodynamics. The 1st Law of Thermodynamics simply states that energy can be neither created nor destroyed (conservation of energy). Thus power generation processes and energy sources actually involve conversion of energy from one form to another, rather than creation of energy from nothing [1][2][4][5].

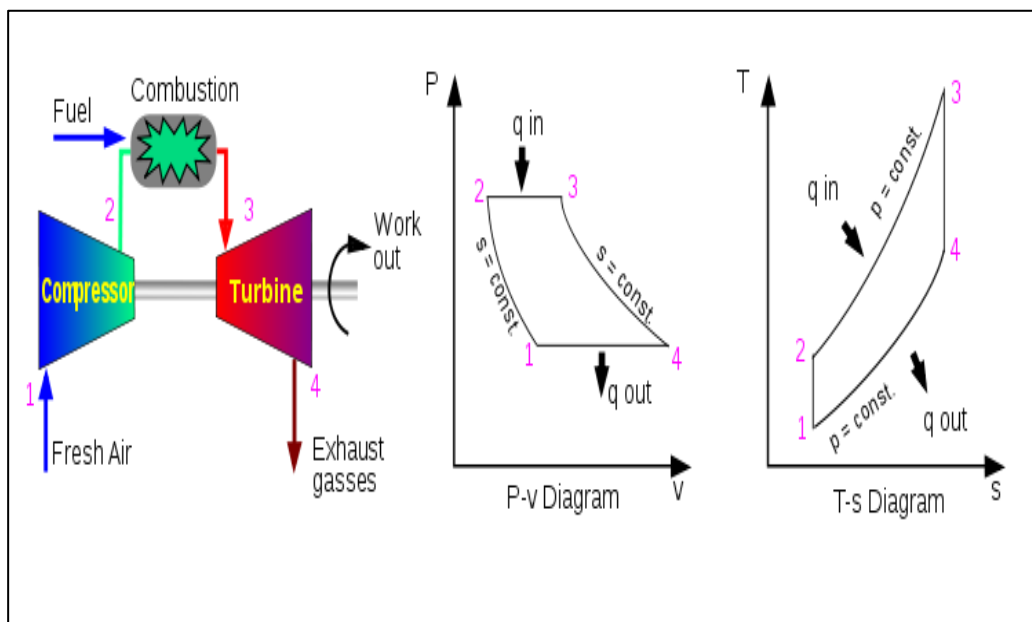


Figure 2.1: Brayton Cycle [1][2]

From Figure 2.1,

Process 1-2: Isentropic compression (in compressor)

Process 2-3: $P = \text{Constant}$ heat addition

Process 3-4: Isentropic Expansion (in turbine)

Process 4-1: $P = \text{Constant}$ heat rejection

2.3 Materials for Gas Turbine Blades

Gas turbine blades are subjected to a very rough environment inside a gas turbine. Factors such as high temperature, high stresses and a potentially high vibration environment affect the performance of the turbine blades. All these factors stated can lead to blade failures, which also can lead to engine failure and that is the main reason why the turbine blades are carefully designed. One of the important factors in manufacturing the early jet engines was the performance of the available materials especially for hot section such as turbine blade. One of the earliest materials used was Nimonic, for British Whittle engines [4][5].



Figure 2.2: Nimonic [4][5]

Furthermore, the development of super alloys in the 1940s and the existence of new processing ways such as vacuum induction melting in the 1950s greatly improved the temperature capability of turbine blades. Then, the introduction of methods such as hot isostatic pressing further improved the alloys used as a material for turbine blades. Nowadays, turbine blades often use nickel-based superalloys that incorporate cobalt, rhenium and chromium [4][5].

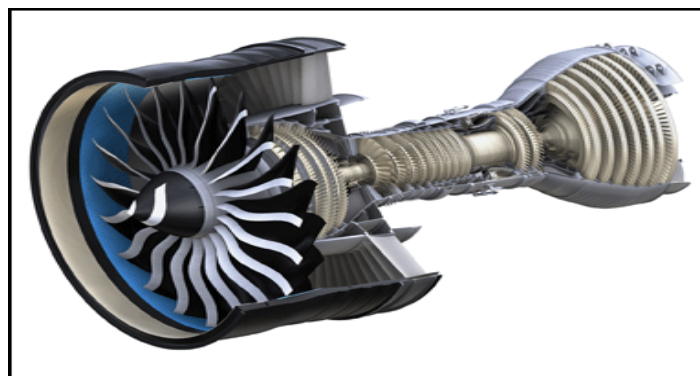


Figure 2.3: Nickel-based superalloys [4][5]

Apart from alloy improvements, a major achievement was the development of single crystal (SC) and directional solidification (DS) production methods. Those introduced method really helpful in increasing the strength against fatigue and creep by aligning the grain boundaries in one direction (DS) or by eliminating grain boundaries all together (SC) [4][5].

Most turbine blades were manufactured by investment casting. One of the important processes involved in investment casting is making a precise negative die of the blade shape that is filled with wax to form the blade shape. A ceramic core in the shape of the passage will be inserted into the middle if the blade is hollow. A heat resistant material will be used to coat the wax blade to make a shell, and then that shell will be filled with the blade alloy. If the middle of the blade is filled with ceramic core, it will be dissolved in a solution that leaves the blade hollow. The blades will be further coated with an TBC followed by the formation of cooling holes, that result in a complete turbine blade [4][5].

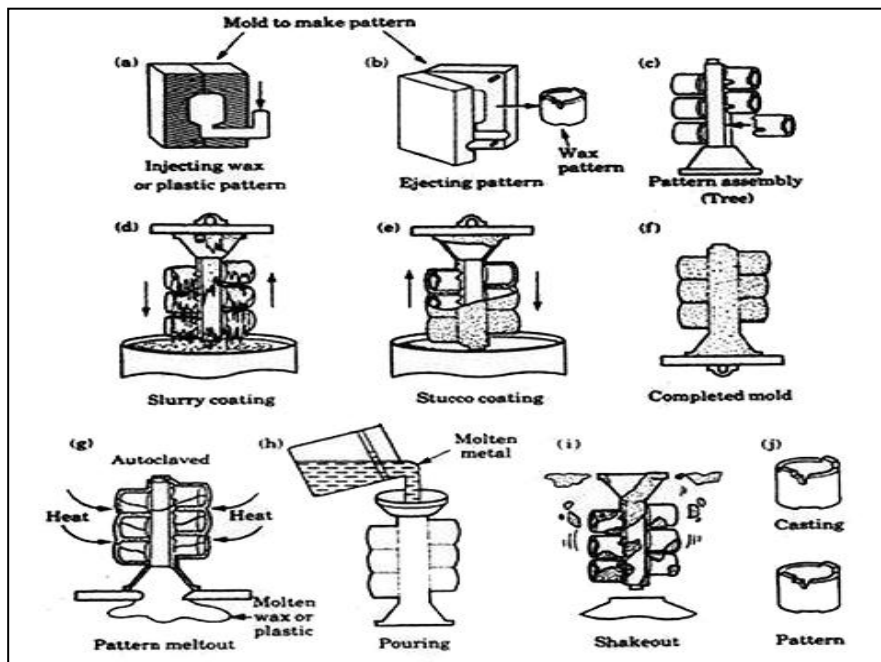


Figure 2.4: Investment Casting [4][5]

2.4 Microstructural aspects of the Nickel base Superalloys components

Superalloys were developed since the second quarter of the 20th century as materials for elevated temperature applications. It can be divided in three main groups: nickel base superalloys, cobalt base superalloys and iron base superalloys. The nickel base alloys are the most widely used. In these alloys, the presence of chromium is essential to assure high-temperature oxidation resistance, whereas other alloying elements are important to guarantee high-temperature strength, especially creep resistance [11].

Other elements such as aluminum and titanium, enable the precipitation of the γ' phase ($\text{Ni}_3(\text{Al,Ti})$) during heat treatment, which strengthens the face centered cubic matrix (γ phase). The γ' precipitates are usually very fine and dispersed and they can be seen only through electron microscopy. Another kind of phase that is also very important for the mechanical properties of nickel base superalloys is carbides. These particles are present in these alloys for two main reasons: because it is very difficult to remove carbon during refining and because carbon is added on purpose to form carbides, which improve creep properties [12].

However, the amount and distribution of carbides must be carefully controlled, otherwise they can cause the occurrence of cracks. The amount of other alloying elements (Cr, Mo, W,) must be high enough to obtain good mechanical and corrosion properties, but low enough to avoid the excessive formation of intermetallic phases which can lead to embrittlement [11,12].

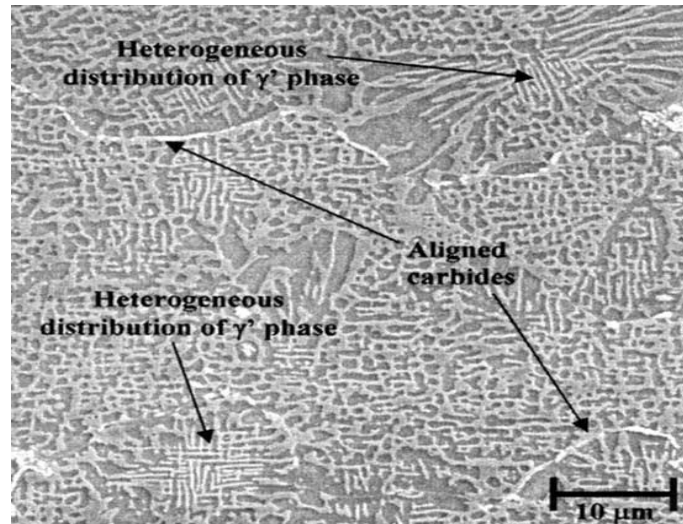


Figure 2.5: Material subjected to overheating [11][12]

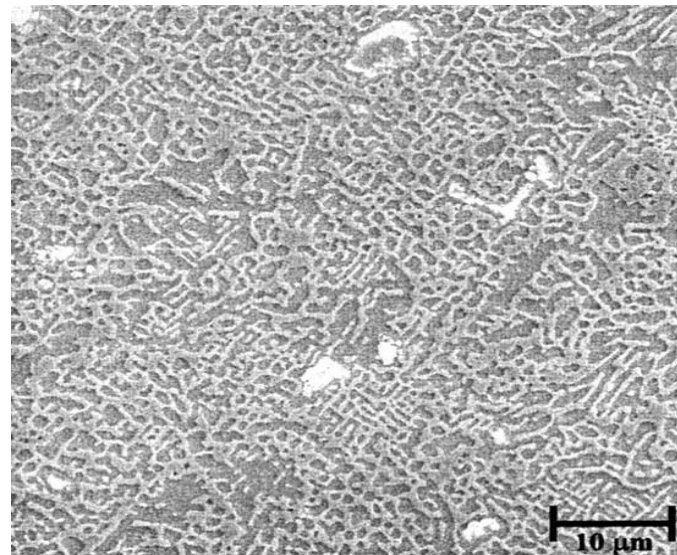


Figure 2.6: Material not subjected to overheating [11][12]

Based on Figure 2.5 and 2.6, it can be seen that the overheated sample 1 presented aligned and connected carbides, which formed preferential sites for nucleation and propagation of cracks. Another important observation was the heterogeneous distribution of phase γ' precipitates, whose segregation is harmful to the mechanical properties of the material. These two factors explain the failure of this component. On the other hand, sample 2, subjected to normal operational conditions, shows a much less heterogeneous matrix than sample 1, not only in relation to γ' precipitates, but also carbides, which, in this case, are much more dispersed throughout the γ matrix [11,12].

2.5 Creep (Deformation)

Creep is known as the tendency of a material to change slowly or deform permanently under the effect of stresses. It is usually affected by a long term exposure to high levels of stress that are below the yield strength of a certain material [3][6][8]. Yield strength is the stress at which a material begins to deform plastically. Below to the yield strength, the material will return to its original shape when the applied stress is removed (deform elastically) but once the yield strength is passed, some fraction of the deformation will be non-reversible and permanent [7]. Creep is always increasing with temperature. Creep will occur fast in materials that are subjected to heat for a long period, and near its melting point [6].

The rate of creep deformation is a function of the material properties, exposure time, applied structural load and exposure temperature. Depending on the magnitude of the applied stress and its period, the failure may become so large that a component can no longer perform its function. For instance, the creep of a turbine blade will cause the blade to contact the casing, lead to the deformation of the blade. Creep is usually concerned by metallurgists and engineers when creating and evaluating components that operates under high stresses or high temperature. Somehow, creep is a deformation mechanism that may or may not be a failure mode. For example, moderate creep in concrete is sometimes welcomed because it relieves tensile stresses that might otherwise lead to cracking [6][7].

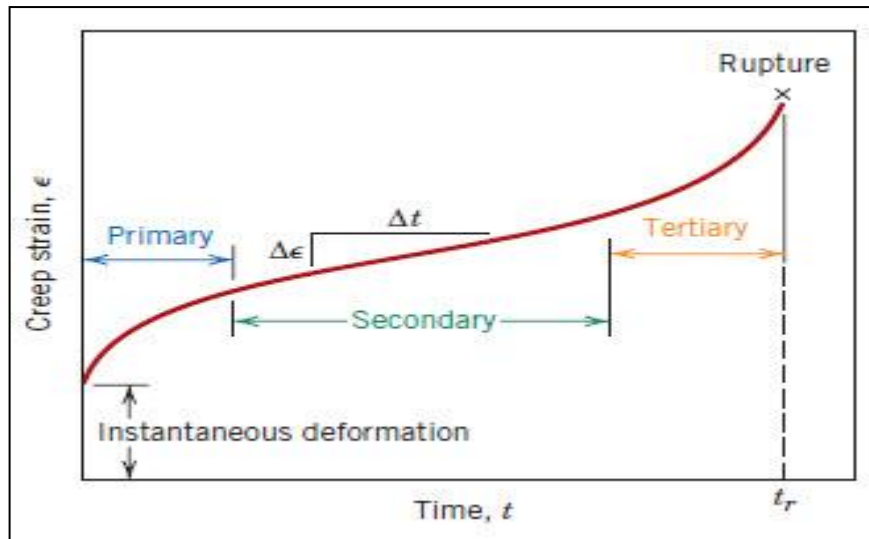


Figure 2.7: Stages of Creep [3][6][7]

Figure 2.7 shows some of the stages involved in creep deformation. During the initial stage, the strain rate is high but will become slower with increasing time. This phenomenon is due to work hardening [8]. Work hardening is the strengthening of a metal by plastic deformation. The dislocation movements within the crystal structure of material is the main causes of the work hardening [9]. Then, the strain rate will reaches a minimum and nearly become a constant. This is normally due to the balance between work hardening and annealing [8]. Annealing is a heat treatment where a material is changed, causing altering in its properties such as ductility and hardness [10]. This stage is known as secondary stage creep. The “creep strain rate” typically refers to the rate in this secondary stage. In tertiary creep, the strain rate increases with stress because of necking phenomena [8]. Necking is a mode of tensile deformation where relatively large amounts of strain localize unduly in a small region of material [9].

2.5.1 Remaining Creep Life Prediction Methods

One of the methods used to predict the remaining creep life is the Stress-Rupture Test (SRT). This method will compute the time to failure of the specimen at certain stress and temperature. Furthermore, it is known as a sudden and complete failure of a material held under a definite constant load for a given period of time at a specific temperature. This test will lead to equations that will be used to obtain the remaining creep life prediction. One of equations is the Larson-Miller Parameter, which in generalized form is:

$$P = T[\log t_r + c] \quad [11]$$

where, T is the operating temperature (K), t_r is the time to rupture (h) and c is the material specific constant often approximated as 20 for most type of metal [11][12]. The experimental data obtain will be extrapolate using this relation.

Another equation that will be used to predict the remaining creep life is the Life Fraction Rule proposed by Robinson [11]. The equation is shown below:

$$\frac{T_s}{T_{rs}} + \frac{t_r}{t_r^*} = 1 \quad [11]$$

$$R.L = T_{rs} - T_s \quad [11]$$

where, T_s is the actual service life of blades (h), T_{rs} is the operational creep life of service-exposed blades (h), t_r is the rupture time of service-exposed blades under accelerated test condition (h), t_r^* is the rupture time of the new materials (unexposed blades) under the same accelerated test conditions (h) and R.L. is the residual life of service-exposed blades (h). [11][12]

CHAPTER 3

RESEARCH METHODOLOGY

3.1 Project Activities

3.1.1 Cutting of sample for Field Emission Scanning Electron Microscope (FESEM) experiment

The process was done at Block 16, UTP with the assists from Mr. Zamil (Lab Technician) using the EDM (Electrical Discharge Machining) Wire Cut Machine. The desired dimension for the sample is 10 mm (height) x 10 mm (width) x 10 mm (length).



Figure 3.1: GE Gas Turbine blades (1st and 3rd Stage)



Figure 3.2: Machine setting process

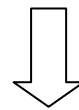


Figure 3.4: The desired sample

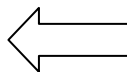


Figure 3.3: The cutting process

There were two samples produced which are from the 1st stage and 3rd stage respectively for microstructure comparison purpose. The different between those samples are the 1st stage sample was taken from the tip outer region (overheated) whereas the 3rd stage sample was taken from the top inner region (normal condition).

The following are the detailed steps taken to cut the sample [11]:

1. The desired dimension was given to the technician. The technician will enter the data on the EDM Wire Cut Machine.
2. A flat metal base was glued to the root of the blade. This is done to ensure that the angle of the blade is 90° to the wire that will cut it.
3. The wire cutting was done based on the dimension desired.
4. The steps were repeated to produce the other sample.

3.1.2 Sample Preparation for the Field Emission Scanning Electron Microscope (FESEM) experiment.

The process was done at Block 17, UTP with the assists from Mr. Mahfuz (Lab Technician).



Figure 3.5: Mounting Process

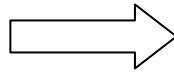


Figure 3.6: Grinding and Polishing process

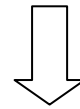


Figure 3.8: Etching process

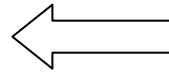


Figure 3.7: Preparation of etching solution

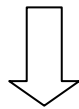


Figure 3.9: Etched sample

The following are the steps to prepare the sample [10]:

1. The sample was mounted by using the Auto Mounting Press machine. The purpose of mounting is to provide a comfortable way to hold the sample while it is being grinded and polished.
2. The sample will be grinded at different grits to achieve a mirror-like image. It was started by using very fine grits until ultra fine grits (P240-P4000).
3. The sandpaper was replaced with polishing cloth and diamond polishing for polishing purpose. The purpose of polishing is to remove the damage introduced by the previous step. Diamond powder is an abrasive material that use to achieve the fastest material removal.
4. Finally, the etching process was done.

Etching

Material of blade: Inconel 738 [10]

Etching Solution: Ni etchant solution [10]

Materials needed: Nitric acid (HNO_3), Acetic acid (CH_3COOH), Sulphuric acid (H_2SO_4), Distilled water, Glass container [10]

Procedure [10]:

1. 100 ml of distilled water was prepared in the glass container.
2. 50 ml of HNO_3 was poured into the glass container followed by 50 ml of CH_3COOH and 20 ml of H_2SO_4 and it was mixed together.
3. The sample was soaked into the solution with mild agitation.
4. The sample was checked by distilled water rinse every 30 seconds or every minute until the Nickel colour was gone.
5. The sample was dried after a thorough distilled water rinse.
6. The preliminary observation was done by using the Optical Microscope.

3.1.3 Field Emission Scanning Electron Microscope (FESEM) experiment

The process was done at Centralized Analytical Lab (CAL), Block P, UTP with the assists from Mr. Anuar (Lab Technologist).



Figure 3.10: Field Emission Scanning Electron Microscope (FESEM)



Figure 3.11: Setting up the FESEM machine



Figure 3.12: Discussion between the lecturer and Graduate Assistor (GA)

3.2 List of Machines and Hardware used

Table 3.1: List of Machines and Hardware used

Machines/Hardware	Function
EDM Wire Cut machine	Used to cut the turbine blades into desired dimension
FESEM	Used to produce microstructure images and chemical composition of the sample
Auto Mounting Press machine	Used to mount the sample to provide a better grip on the sample
Grinding machine	Used to produce a mirror-like image
Polishing machine	Used to remove the damage introduced by grinding process
Ni etchant solution	Used to produce the perfect surface for FESEM examination

3.3 Flow of the Project

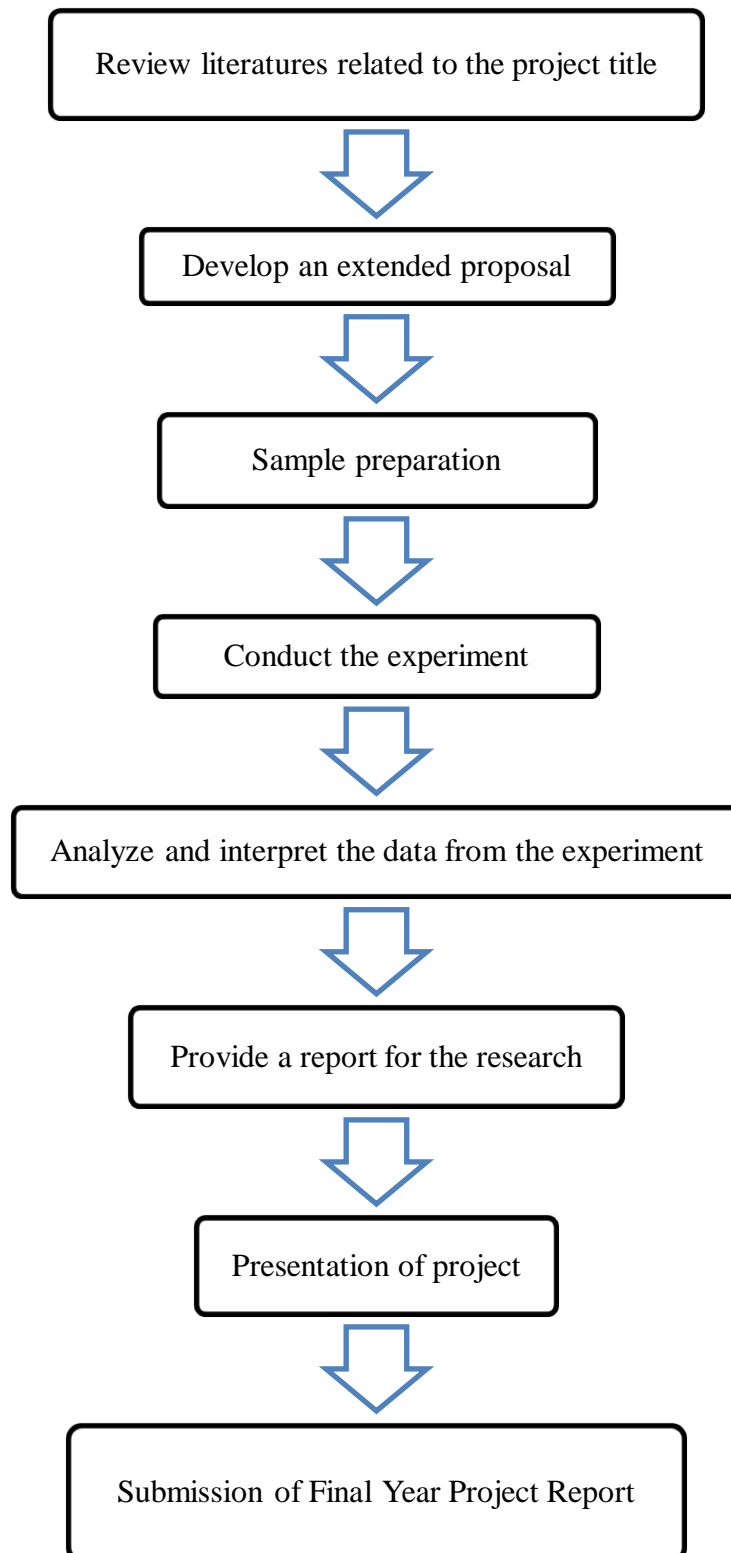


Figure 3.14: Flow of the Project

3.4 Experimental Procedures

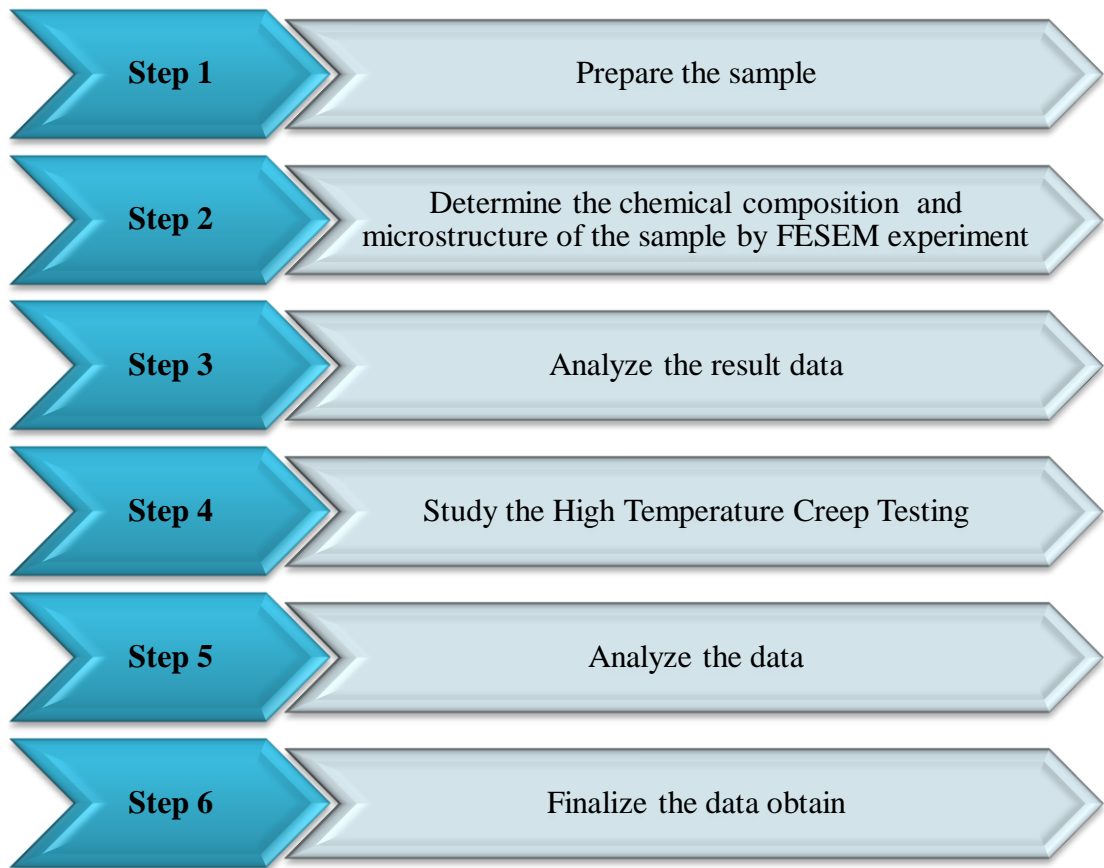


Figure 3.15: Experimental procedures

3.5 Gantt Chart & Key-Milestones for FYP I

Table 3.2: Gantt Chart & Key-Milestones for FYP I

No.	Details	Weeks														
		1	2	3	4	5	6	7	MID SEMESTER BREAK	8	9	10	11	12	13	14
1	Consolidation of FYP Topics								MID SEMESTER BREAK							
2	Topic assignments to students								MID SEMESTER BREAK							
3	Research for the topic assigned								MID SEMESTER BREAK							
3	Preparation for Extended Proposal								MID SEMESTER BREAK							
4	Submission of Extended Proposal						★		MID SEMESTER BREAK							
5	Research for the experimental procedure and work								MID SEMESTER BREAK							
6	Research for the material properties								MID SEMESTER BREAK							
7	Preparation for Proposal Defence								MID SEMESTER BREAK							
8	Proposal Defence								MID SEMESTER BREAK	★						
9	Preparation for Interim Report								MID SEMESTER BREAK							
10	Submission of Interim Report								MID SEMESTER BREAK							★

Legends:

Process

Key Milestones ★

3.6 Gantt Chart & Key-Milestones for FYP II

Table 3.3: Gantt Chart & Key-Milestones for FYP II

No.	Details	Weeks															
		1	2	3	4	5	6	7	MID SEMESTER BREAK	8	9	10	11	12	13	14	
1	Lab Bookings	■	■														
2	Appointment with Lab Technician	■	■														
3	Cutting the Sample			■	■												
3	Sample Preparation for FESEM experiment					■	■	■									
4	FESEM experiment									■							
5	Submission of Progress Report										★						
6	High Temperature Creep Testing Experiment										■	■	■	■			
7	Poster Submission															★	
8	Submission of Dissertation (softbound)															★	
9	Submission of Technical Paper																★
10	Oral Presentation (Viva)																★
11	Submission of Dissertation (hardbound)																★

Legends:

Process 

Key Milestones 

CHAPTER 4

RESULTS & DISCUSSION

Results and discussion can be divided into two parts:-

- a. Field Emission Scanning Electron Microscope (FESEM)
 - i. 1st Stage of used Gas Turbine Blade (Overheated)
 - ii. 3rd Stage of used Gas Turbine Blade (Normal Condition)
- b. Stress-Rupture test analysis

4.1 Field Emission Scanning Electron Microscope (FESEM)

This experiment was done to investigate the microstructure arrangement and the chemical composition of the sample at different stage of used gas turbine blade.

a. i. 1st Stage of used Gas Turbine Blade Microstructure

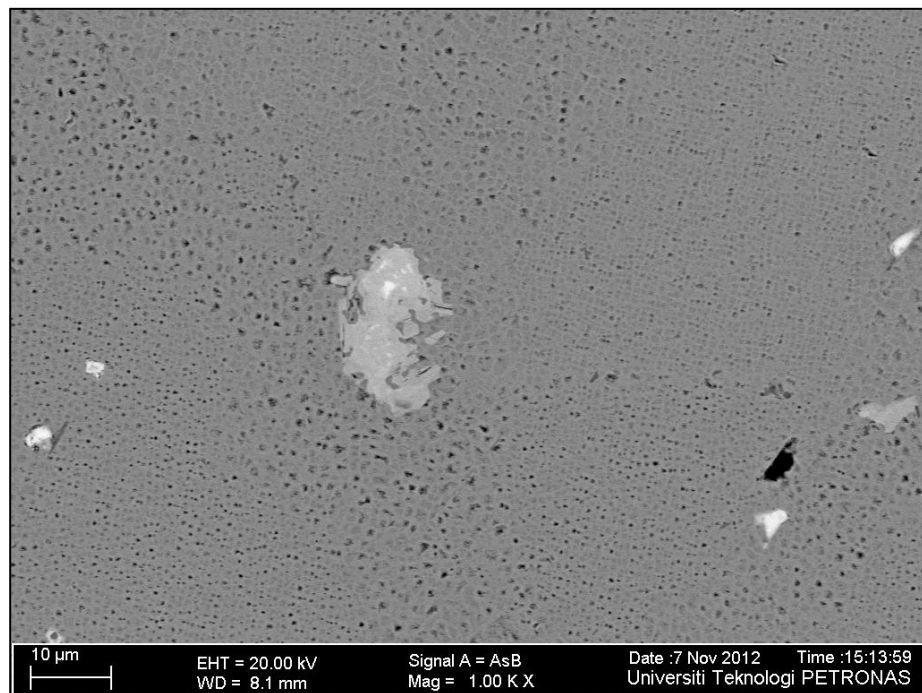


Figure 4.1:1st Stage of used Gas Turbine Blade at 1.0 K X magnification

Based on Figure 4.1, it is very clear that the 1st Stage used Gas Turbine blade (overheated), presented aligned and connected carbides, which formed preferential sites for nucleation and propagation of cracks [11].

Other than that, another important observation was the heterogeneous distribution of phase Cobalt (Co) precipitates, whose segregation is harmful to the mechanical properties of the material. Furthermore, the coarsened gamma (γ) size is in the range of 0.5–2 μm in this section. The large size coarsened γ precipitates are surrounded by the γ denuded zone (darker regions), devoid of secondary γ precipitates.

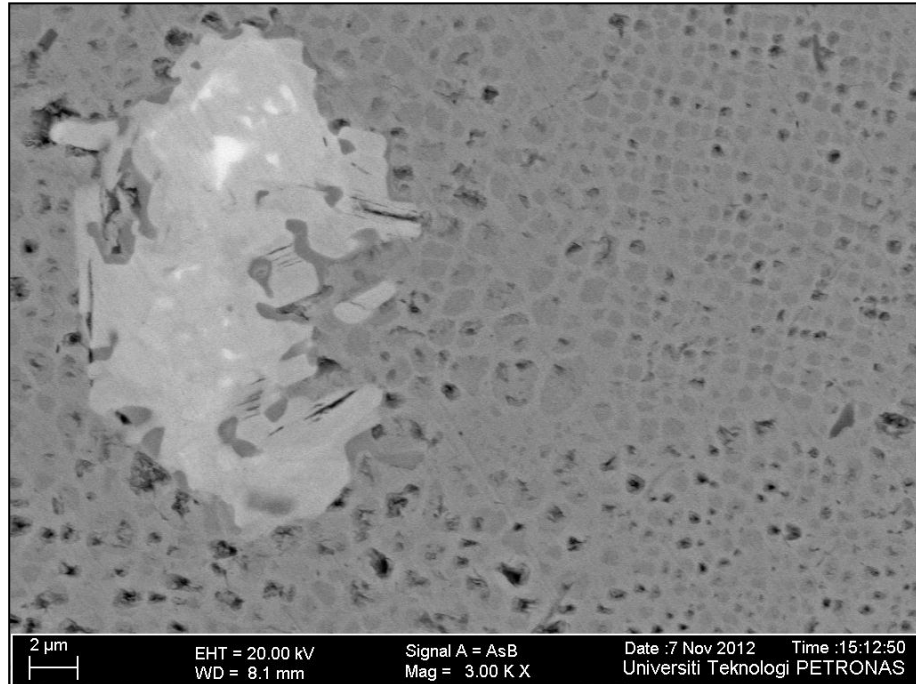


Figure 4.2:1st Stage of used Gas Turbine Blade at 3.0 K X magnification

Figures 4.2 show carbides precipitation in grain boundaries that is represented in the formation of continuous films (including 13.24 percent Cr) and dispersed particles (include 6.81 percent Ti) of carbides, respectively. Carbides precipitation results in decreasing of alloy ductility and toughness [11]. Figure 4.2 show a material in the middle stage of secondary creep. The “creep strain rate” typically refers to the rate in this secondary stage [8]. Furthermore, there were a large number of cracks at different regions of blades because of operation at high temperatures and stresses over a long period of time. Some of these cracks are shown in Figures 4.2. In Figure 4.2, the author observed an intergranular crack on fracture surface. The appearance of the fracture surface resembles a dimple-like fracture. The dimple-like appearance can be attributed to the microcavities, which could be related to intergranular decohesion of carbides [12]. These microcavities serve as the origin of a creep failure mechanism. Also, the author observed an intergranular crack on the 1st stage blade coating and several intergranular cracks that were located on transverse section

of the blade surface (Figure 4.2). The coating crack initiation was probably due to a thermal fatigue mechanism, as a result of high thermal transient loads and crack grain boundary initiation and propagation in the substrate by a creep mechanism (high steady state loads) [11][12].

ii. 1st Stage of used Gas Turbine Blade Chemical Composition

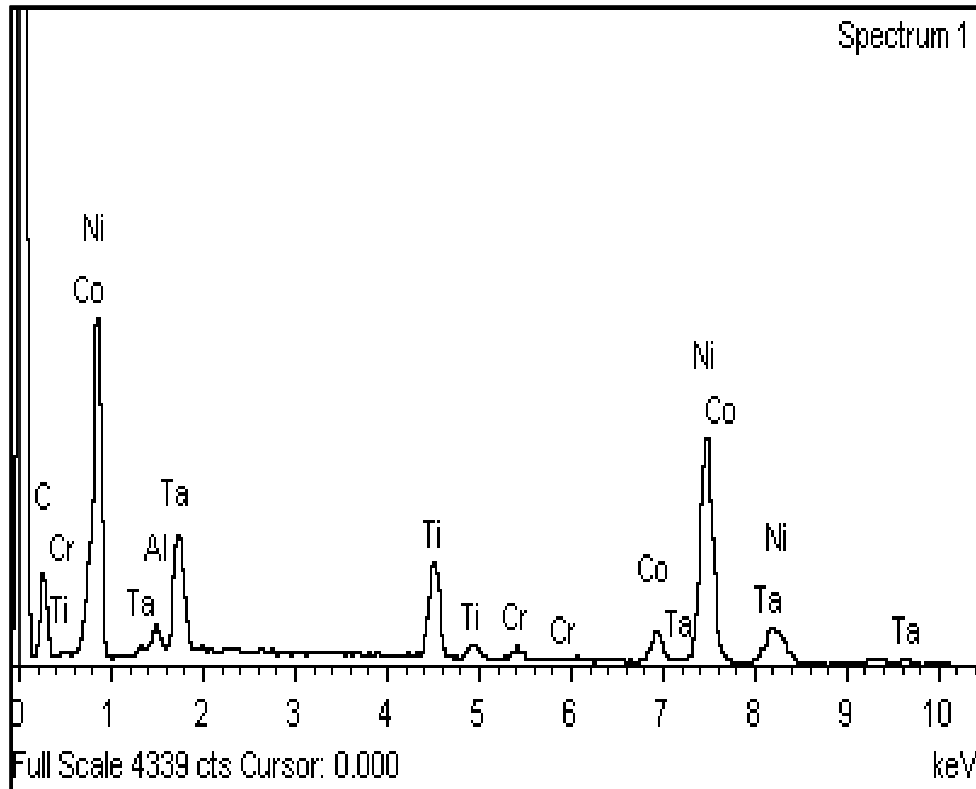


Figure 4.3:1st Stage of used Gas Turbine blade Chemical Composition

Based on Figure 4.3, the major elements in the blades are Nickel, giving an initial judgment that the blade is made of Nickel-based superalloys. Then, further study was done; comparing the result obtained from FESEM examination with literatures. Finally, it has been concluded that the type of alloy used to fabricate the blades is Inconel 738 [10]. Inconel 738 offers a combination of outstanding high-heat creep rupture strength and corrosion resistance. It is also better than many high-strength superalloys with lower chromium content. The nickel-based alloys are vacuum-cast and precipitation-hardened, offering exceptional mechanical properties. Inconel 738 holds up to the hot corrosive environments found in the gas turbine industry [10].

Based on Table 4.1, it can be justified that Nickel is the major element inside the 1st stage used gas turbine blade. The blade was made up of approximately 42.13 % percent of Nickel. Nickel is a chemical element with the symbol Ni and atomic number 28. It is a silvery-white lustrous metal with a slight golden tinge. Nickel belongs to the transition metals and it is hard and ductile [11]. The least element was Tantalum with 0.95%. Tantalum is also a chemical element with the symbol Ta and atomic number 73. Tantalum is a hard, blue-gray, lustrous transition metal that is highly corrosion resistant [11]. Another major element inside the blade is Carbon (31.01%). These particles are present in these alloys for two main reasons: because it is very difficult to remove carbon during refining and because carbon is added on purpose to form carbides, which improve creep properties [12].

Table 4.1: 1st Stage of used Gas Turbine blade
Tabulated Chemical Composition

Element	Weight%	Atomic%
C K	31.01	70.65
Al K	1.10	1.11
Ti K	6.81	3.89
Cr K	13.24	2.00
Co K	4.75	2.21
Ni K	42.13	19.64
Ta M	0.95	0.50
Totals	100.00	

b. i. 3rd Stage of used Gas Turbine Blade Microstructure

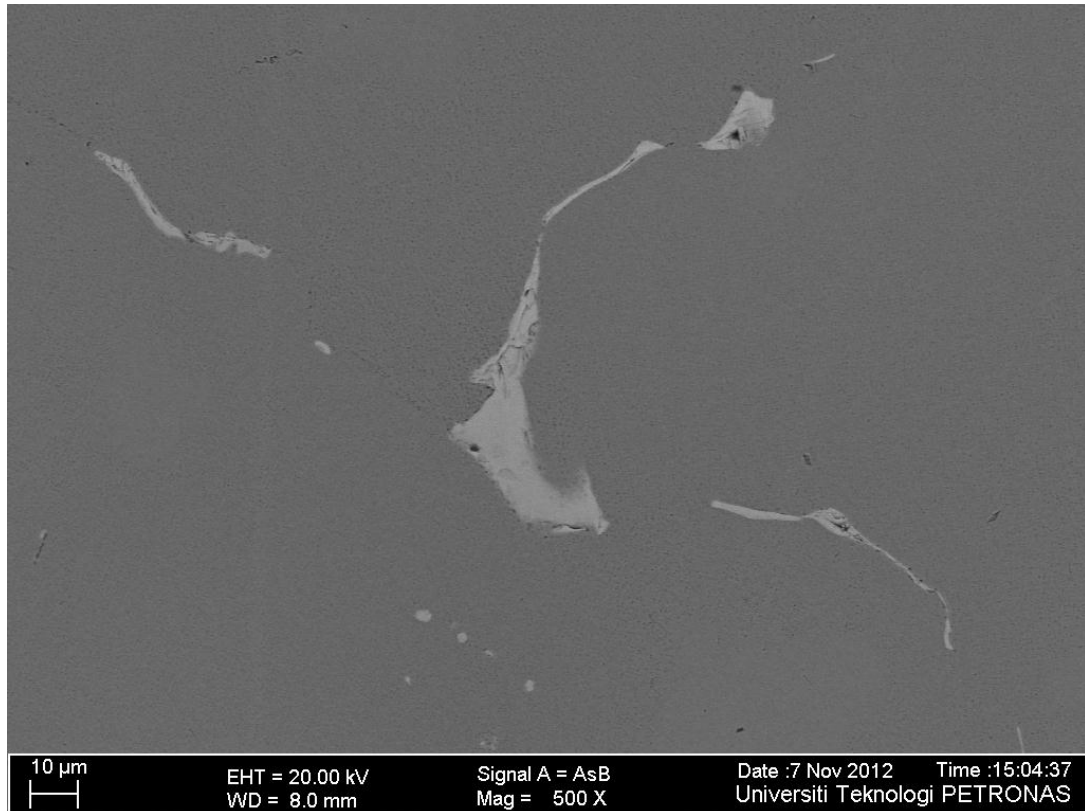


Figure 4.4:3rd Stage of used Gas Turbine blade at 500 X magnification

Based on Figure 4.4, 3rd stage used Gas Turbine blade (normal condition), it shows a much less heterogeneous matrix than sample 1, not only in relation to Cobalt (Co) precipitates, but also carbides, which, in this case, are less dispersed throughout the gamma (γ) matrix [11]. Co precipitates segregation is harmful to the mechanical properties of the material. In addition, the carbides precipitation in grain boundaries that is represented in the formation of continuous films is not that much compared to the 1st stage blade (including 8.14 percent Cr) and dispersed particles (include 2.47 percent Ti) of carbides, respectively. Carbides precipitation will result to intergranular corrosion. This situation can happen in corrosion-resistant alloys, when the grain boundaries are depleted, known as grain boundary depletion, of the corrosion-inhibiting elements such as Chromium. This mechanism is called sensitization. Carbides precipitation would also results in decreasing of alloy ductility and toughness [11].

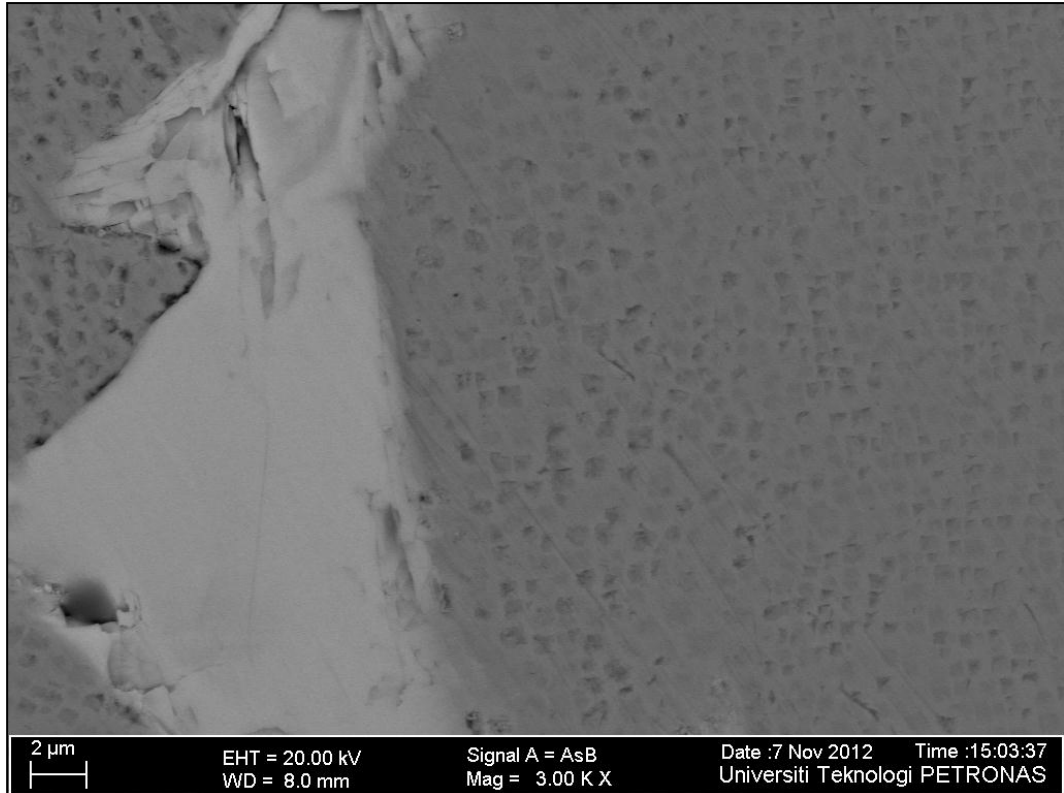


Figure 4.5:3rd Stage of used Gas Turbine blade at 3.00 K X magnification

Based on Figure 4.5, cracks and fracture seems just begin to develop as it cannot be clearly seen compared to the other sample in Figure 4.2. This shows that the 3rd stage blade was not subjected to high stress and temperature experienced by the 1st stage blade. But still, there were stress and temperature that affect the performance of the 3rd stage blade. Based on Figure 4.5, it shows that the grain boundaries are begin to coarse as a result of creep effect in a high stress and temperature inside a gas turbine. But, it cannot be clearly seen as it is still in the early stage of secondary creep. The “creep strain rate” typically refers to the rate in this secondary stage [8]. Other than that, the cracks are begin to develop as a result of centrifugal force inside the turbine. In addition, it is also affected by the operation at high temperatures and stresses over a long period of time. The large white portion can be attributed to the microcavities, which could be related to intergranular decohesion of carbides. These microcavities serve as the origin of a creep failure mechanism [11][12].

ii. 3rd Stage of used Gas Turbine Blade Chemical Composition

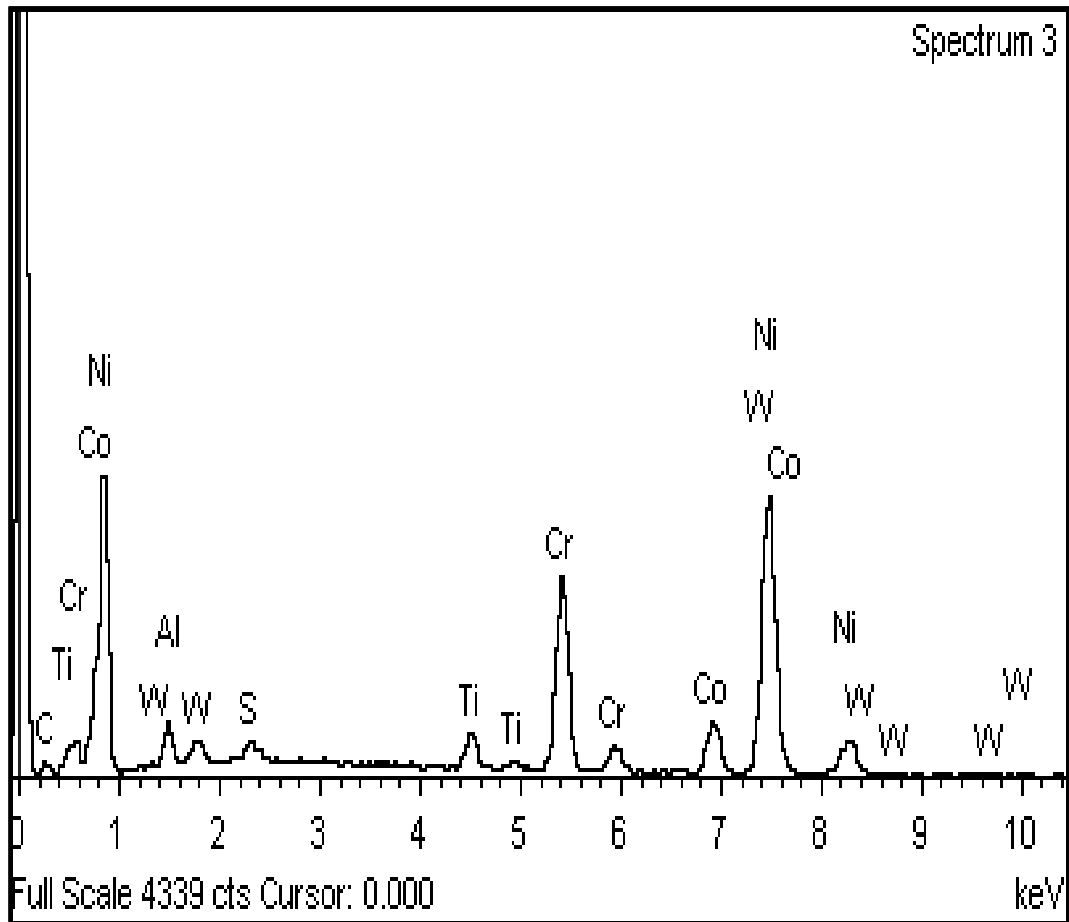


Figure 4.6:3rd Stage of used Gas Turbine blade Chemical Composition

Based on Figure 4.6, the major elements in the blades are Nickel, which support the judgment that the blade is made of Nickel-based superalloys. This is supported by the comparison between the results obtained from FESEM examination with literatures. It had been conclude that the material used to manufacture the blade is Inconel 738. Inconel 738 offers a combination of outstanding high-heat creep rupture strength and corrosion resistance. It is also better than many high-strength super alloys with lower chromium content. The nickel-based alloys are vacuum-cast and precipitation-hardened, offering exceptional mechanical properties. Inconel 738 holds up to the hot corrosive environments found in the gas turbine industry [10].

Based on Table 4.2, once again that it can be clearly seen that Nickel is the major element inside the 1st stage used gas turbine blade. The blade consists of approximately 55.91 % percent of Nickel. The least element was Tantalum with 0.61%. Still the second largest portion is Carbon (18.17%). These particles are present in these alloys for two main reasons: because it is very difficult to remove carbon during refining and because carbon is added on purpose to form carbides, which improve creep properties [12].

Table 4.2: 3rd Stage of used Gas Turbine blade

Tabulated Chemical Composition

Element	Weight%	Atomic%
C K	18.17	29.14
Al K	2.80	4.46
Ta K	0.61	0.82
Ti K	2.47	2.22
Cr K	8.14	15.04
Co K	9.20	6.72
Ni K	55.91	40.97
Totals	100.00	

Table 4.3 shows the tensile properties of Inconel 738. It shows that the Elastic Modulus is 110 GPA, Yield Strength is 950 MPa, and Ultimate Tensile Strength is 1100 MPa [13][14].

Table 4.3: Tensile properties of Inconel 738 [13][14]

Property	Inconel 738
Elastic Modulus (GPa)	110
Yield Strength (MPa)	950
Ultimate Tensile Strength (MPa)	1100

4.2 Stress-Rupture test analysis

Since the High Temperature Creep Testing Machine (HTCTM) is not available, analysis of journals and literature had been made. An important information that the author gathered is the blades had been used for 70 000 hours before being sent to UTP for the remaining creep life prediction purpose. After concluding the type of material for the blades which is Inconel 738, further research had been done on previous Stress-Rupture test using Inconel 738 as a sample. Based on the research obtained, extrapolation of data had been carried out that lead to the following result.

4.2.1 Stress-Rupture test

Stress-Rupture test is widely used in estimation of creep life of high temperature materials instead of usual creep test because it does not need long periods of time and it gives a good indication about creep behaviour of materials [12]. The result obtain in this research is preliminary. A real Stress-Rupture test should be done to gain a more reliable result. Table 4.4 show the Stress-Rupture test analysis.

Table 4.4: Stress-Rupture test analysis

Actual service life of blades (h)	Test Condition (MPa)		Time to rupture (h)
	Stress (MPa)	Temperature (°C)	
Unexposed	400	850	602
	500	850	311
	600	850	98
60 000	400	850	180
	500	850	94
	600	850	32
70 000	400	850	118
	500	850	60
	600	850	20
80 000	400	850	53
	500	850	27
	600	850	10

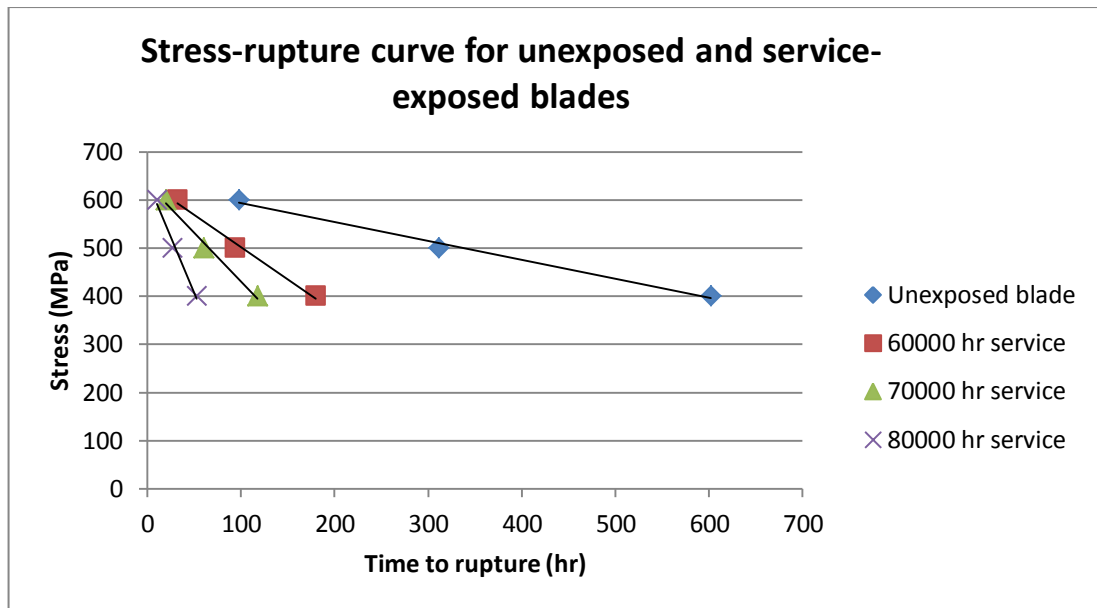


Figure 4.7: Stress-Rupture curve

Based Figure 4.7, it can be clearly seen that the higher the service hour, the shorter the time taken to rupture. The unexposed blade showed a different pattern of graph compared to the other service blade. It is less steeper compared to the other that shows its' rupture time is very slow.

4.2.2 Remaining Creep Life Prediction

The remaining creep life prediction of blade was done using two different methods:

- i. Larson-Miller parameter
- ii. Life Fraction Rule

4.2.2.1 Larson-Miller parameter

The Larson-Miller parameter equation is given below:

$$P = T[\log t_r + c] \quad [11]$$

where, T is the operating temperature (K), t_r is the time to rupture (h) and c is the material specific constant often approximated as 20 for most type of metal [11][12].

Table 4.5 show the result from Stress-Rupture test analysis that had been further developed based on the Larson-Miller equation.

Table 4.5: Larson-Miller analysis

Actual service life of blades (h)	Temperature (K)	Log t_r (h)	C	Larson-Miller Parameter
Unexposed	1 123	2.78	20	25 581.94
	1 123	2.49	20	25 256.27
	1 123	1.99	20	24 694.77
60 000	1 123	2.25	20	24 986.75
	1 123	1.97	20	24 672.31
	1 123	1.51	20	24 155.73
70 000	1 123	2.07	20	24 784.61
	1 123	1.78	20	24 458.94
	1 123	1.30	20	23 919.90
80 000	1 123	1.72	20	24 391.56
	1 123	1.43	20	24 065.89
	1 123	1.00	20	23 583.00

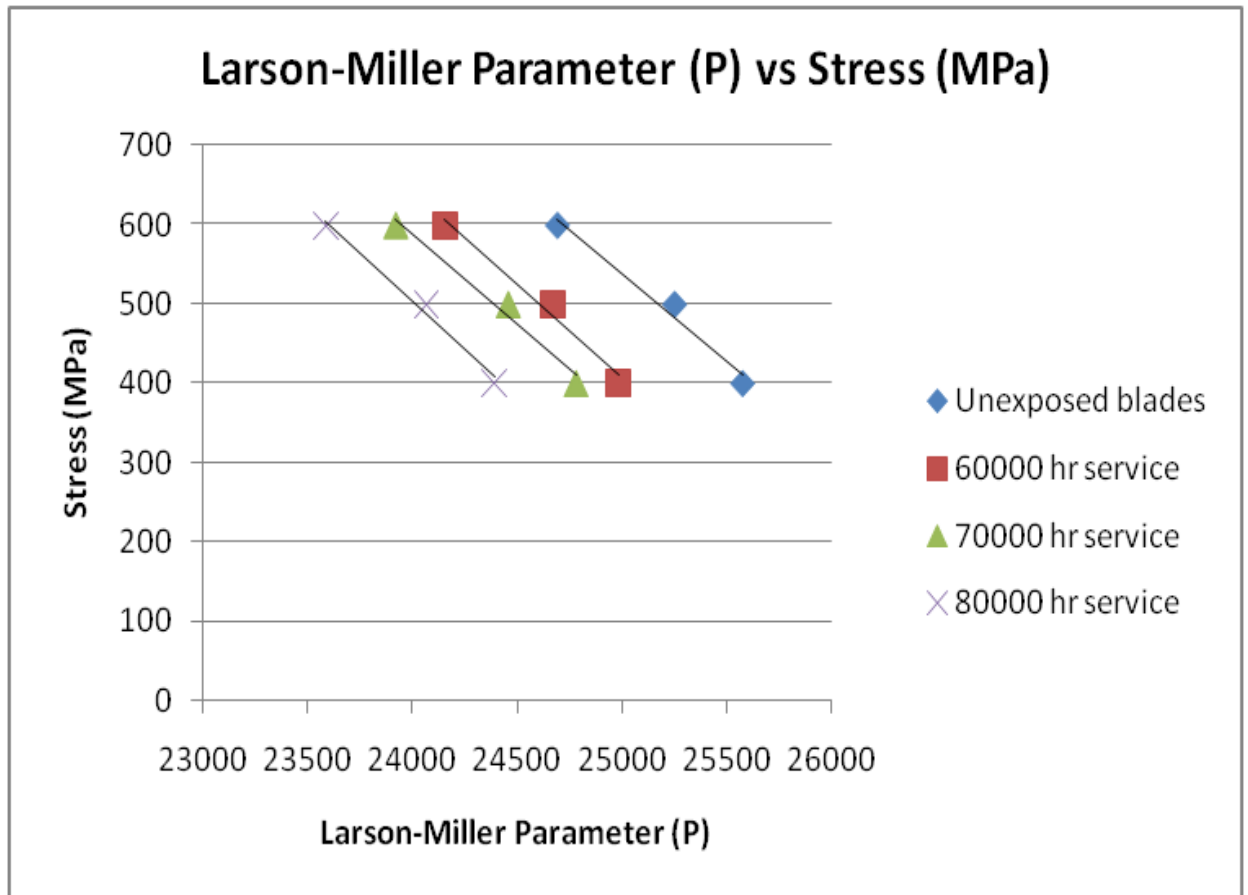


Figure 4.8: Larson-Miller parameter for unexposed and exposed blades

Based on the Figure 4.8, it can be seen that Larson-Miller parameter is increasing as service hour is decreasing. Usually, the manufacturer will mention the Larson-Miller parameter value for the blades that they supplied to make its' easier to predict the remaining life of the blades. But unfortunately, not all the information is correct. So, the data obtain from the Stress-Rupture test is more reliable to predict the remaining creep life of the blades. For an example, the LMP value at stress equals to 550 MPa for 60 000 hour service blades is 24 829.53. By taking temperature (T) to be equal to 850°C as a constant value throughout the study, we can calculate the data to obtain the time to rupture. The result will yield approximately 128 hours. This value will be further used in life fraction rule to obtain the remaining creep life prediction of the blade.

4.2.2.2 Life Fraction rule

The Life Fraction rule equation is given below:

$$\frac{T_s}{T_{rs}} + \frac{t_r}{t_r^*} = 1 \quad [11]$$

$$R.L = T_{rs} - T_s \quad [11]$$

where, T_s is the actual service life of blades (h), T_{rs} is the operational creep life of service-exposed blades (h), t_r is the rupture time of service-exposed blades under accelerated test condition (h), t_r^* is the rupture time of the new materials (unexposed blades) under the same accelerated test conditions (h) and R.L. is the residual life of service-exposed blades (h) [11][12]. The result from the Stress-Rupture test analysis had been further developed based on the Life Fraction rule equation. This is shown in Table 4.6.

Table 4.6: Life Fraction rule analysis

Actual service life of blades (h)	Test Condition (MPa)		Operational creep life (h)	Residual life (h)
	Stress (MPa)	Temperature (°C)		
60 000	400	850	86205	26 205
	500	850	85206	25 206
	600	850	86470	26 470
70 000	400	850	87066	17 066
	500	850	86733	16 733
	600	850	87949	17 949
80 000	400	850	87723	7 723
	500	850	87605	7 605
	600	850	89090	9 090

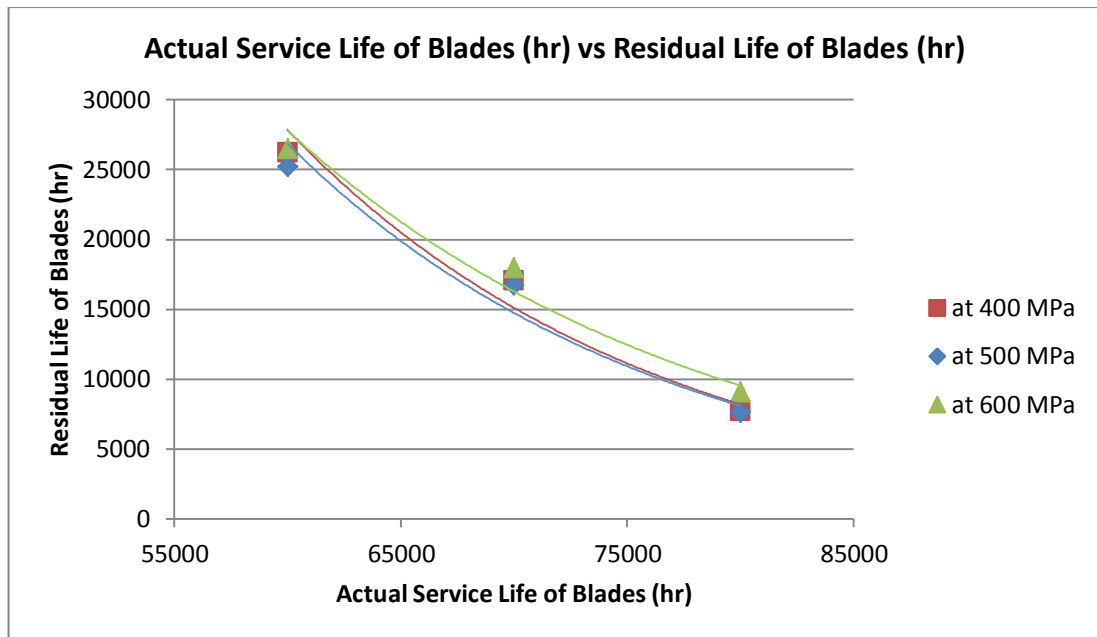


Figure 4.9: Relationship between actual service life and residual life of service-exposed blades

Based on Figure 4.9, it can be clearly seen that the blade from MLNG, Labuan still can be used for more than a year based on its operating stress (MPa) while the temperature is kept constant. Changing the blade while it still can be used would be a waste of capital cost on new blade replacement. So, it is very important to do a proper study on the remaining creep life prediction of used gas turbine blades. Furthermore, the graph plotted shows that as the operating stress and actual service life of blades increase, the residual life of blades will decrease. The main cause of this condition is that the microstructure changes that could not withstand the high stress and temperature condition inside the gas turbine. This will lead to slow deformation which is known as creep. Creep is the tendency of a material to change slowly or deform permanently under the effect of stresses. It is usually affected by a long-term exposure to high levels of stress that are below the Yield Strength of a certain material such as gas turbine blades [3][6][8]. The Yield Strength of Inconel 738 is 950 MPa. After all, the result obtained in this project is preliminary thus Stress-Rupture tests have to be carried out to improve the outcome.

CHAPTER 5

CONCLUSION AND RECOMMENDATIONS

5.1 Conclusion

In conclusion, the author managed to achieve the objective of the study. The main objective of the study was to predict the remaining creep life of used gas turbine blades. As we all known, turbine blades is expensive and costly material. In order to save capital cost, it is very important to know when will the blade reach its' deform state without believing 100% to the information given by the manufacturer. This will also ensure that the blade will not be change earlier or too late. By conducting the research, the author managed to have a preliminary result on remaining creep life prediction of the used gas turbine blade supplied by MLNG, Labuan. With the application of Larson-Miller parameter and Life Fraction rule, the author had found out that the supplied blade still can be used for more than a year based on its' operating stress and temperature inside the gas turbine. Besides that, two different sample which are 1st stage used gas turbine blade (overheated) and 3rd stage used gas turbine blade (normal operation) were compared based on metallurgical analysis. It had been found out that the 1st stage used gas turbine blade (overheated) suffer more compared to the 3rd stage used gas turbine blade (normal operation) from several microstructure changes, which affect their function. They are formation of cracks, fractures and coarsening of grain boundaries on the material as a result from high stress and temperature condition. Lastly, the author hopes that the Stress-Rupture test can be carried out by using the High Temperature Creep Testing Machine (HTCTM) in the future to obtain a more reliable result.

5.2 Recommendations

If the experiment can be conducted in the future, it is very important to examine the microstructure after the Stress-Rupture test had been carried out. This will draw a comparison between the microstructure before and after the blade has ruptured. Furthermore, the chemical composition could also be compared. This will lead to a more precise result. Besides that, Stress-Rupture test will take a lot of time. It might take a month or more to obtain the result since the samples need to reach its rupture time under different operating stress. In addition, sample preparation for both microstructure and Stress-Rupture test will take some time. So, the best thing is to start earlier and have a fix guideline that must be obeyed to avoid any delay. Since the High Temperature Creep Testing Machine (HTCTM) is not available in UTP, it is very important to contact the person who can help to perform Stress-Rupture test as earlier as possible. Reservation should be made earlier to avoid complication in the future. Besides that, always keep in touch with respective supervisor. The author hope that the preliminary result could be modify in the future after the Stress-Rupture test had been perform.

CHAPTER 6

REFERENCES

- [1] H.I.H. Saravanamuttoo, G.F.C. Rogers and H. Cohen, 2001, Gas Turbine (5th ed.) Theory Pearson Education.

- [2] Boyce, Meherwan P., 2006, Chapter 9: Axial Flow Turbines, Chapter 11: Materials, Gas Turbine Engineering Handbook (3rd ed.), Oxford, Elsevier.

- [3] Frost, Harold J., Ashby, Michael F, 1982, Deformation-Mechanism Maps: The Plasticity and Creep of Metals and Ceramics, Pergamon Press.

- [4] John Molloy, 1998, Forensic Investigation of a Gas Turbine Event, M&M Engineering.

- [5] Schilke, P. W., 2004, Advanced Gas Turbine Materials and Coatings. GE Energy.

- [6] Ashby, Michael F., Jones, David R. H., 1980, Engineering Materials 1: An Introduction to their Properties and Applications, Pergamon Press.

- [7] Beer, Ferdinand P., Johnston, E. Russell, Dewolf, John T., 2001, Mechanics of Materials (3rd ed.). McGraw-Hill.

- [8] Smith, William F., Hashemi, Javad, 2006, Foundations of Materials Science and Engineering (4th ed.), McGraw-Hill.

- [9] Degarmo, E. Paul, Black, J T., Kohser, Ronald A., 2003, Materials and Processes in Manufacturing (9th ed.), Wiley.

- [10] Van Vlack, L.H., 1985, Elements of Materials Science and Engineering, Addison-Wesley.

- [11] Walls, D.P., Delaneuville, R.E., and Cunningham, S.E., 1997, Damage Tolerance Based Life Prediction in Gas Turbine Engine under Vibratory High Cycle Fatigue, *Journal of Engineering for Gas Turbines and Power*, vol. 119, 1997, pp. 143–6.
- [12] Burns, J., 1998, Gas Turbine Engine Blade Life Prediction for High Cycle Fatigue, The Technical Cooperation Program (TTCP), P-TP1.
- [13] Hertzberg, Richard W., 1996 *Deformation and Fracture Mechanics of Engineering Materials*, Fourth Edition. John Wiley and Sons, Inc., Hoboken, NJ.
- [14] Larson, F.R.; and Miller, James: A Time-Temperature Relationship for Rupture and Creep Stresses. *Trans. ASME*, vol. 74, pp. 765–775.
- [15] B. Walser, September 1979, *Proceedings of Conference on Heat and Mass Transfer in Metallurgical System*, Yugoslavia, p. 673.
- [16] C. Barbosa, J.L. Nascimento, I.M.V. Caminha, I.C. Abud, September 2003 *Acta Macroscopica*.
- [17] Y. Xu, J.L. Bassani, 1999, *Mater. Sci. Eng. A260*.
- [18] R. Castillo, A.K. Koul, E.H Toscano, 1987, *J. Eng. Gas Turbines Power*.
- [19] R. Castillo, A.K. Koul, 1986, *Proceedings of Conference on High Temp. Alloys for Gas Turbine & Other Applications*, Belgium.
- [20] M.A Meyers, K.K. Chawla, 1999, *Mechanical Behaviours of Materials*, Prentice-Hall International Inc.

CHAPTER 7

APPENDICES

7.1 Field Emission Scanning Electron Microscope (FESEM)

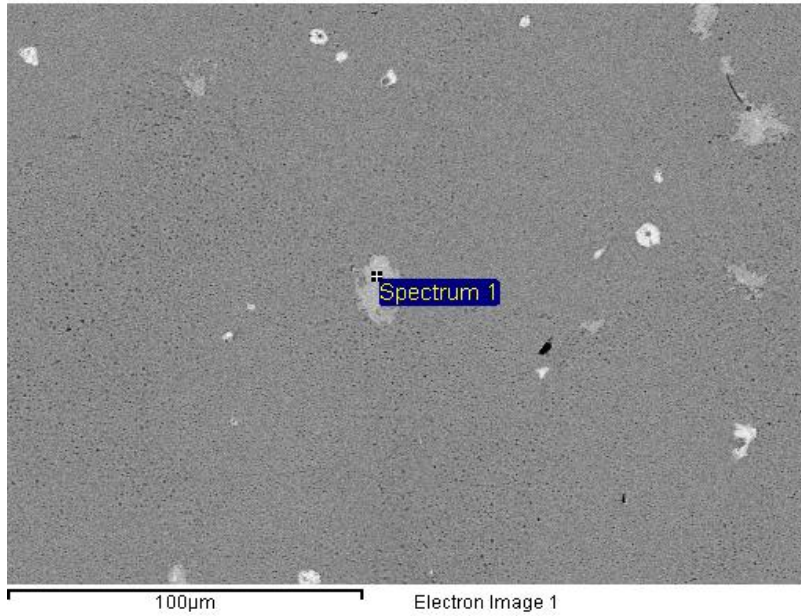


Figure 7.1: 1st Stage of used Gas Turbine blade Electron Image

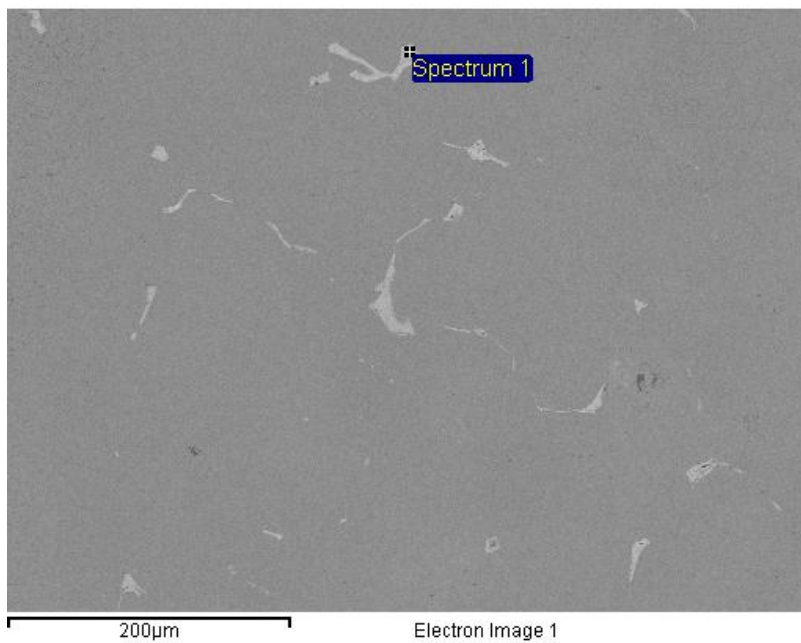


Figure 7.2: 3rd Stage of used Gas Turbine blade Electron Image

7.2 High Temperature Creep Testing Machine (HTCTM)



Figure 7.3: High Temperature Creep Testing Machine (HTCTM) [12]

7.3 Creep Life Prediction Method

For 70 000 hours service blade, Stress (σ) applied = 600 MPa

7.3.1 Larson-Miller Parameter

Given,

$$T = 850 \text{ }^\circ\text{C}$$

$$= 850 + 273$$

$$= 1123 \text{ K}$$

$$t_r = 20 \text{ h}$$

$$C = 20$$

$$P = T[\log t_r + c]$$

$$P = 1123 (\log 20 + 20)$$

$$\mathbf{P = 23\ 919.90}$$

7.3.2 Life Fraction Rule

Given,

$$T_s = 70\ 000 \text{ h}$$

$$T_{rs} = ?$$

$$t_r = 20$$

$$t_r^* = 98$$

$$\frac{T_s}{T_{rs}} + \frac{t_r}{t_r^*} = 1$$

$$\frac{70\ 000}{T_{rs}} + \frac{20}{98} = 1$$

$$\frac{70\ 000}{T_{rs}} = 1 - 0.204$$

$$T_{rs} = 87\ 949$$

$$R.L = T_{rs} - T_s$$

$$R.L = 87\ 949 - 70\ 000$$

$$\mathbf{R.L = 17\ 949 \text{ hours}}$$